EMPLACEMENT OF FAHRENHEIT CRATER EJECTA AT THE LUNA-24 SITE

MARK SETTLE, MARK J. CINTALA, and JAMES W. HEAD
Dept. of Geological Sciences, Brown University, Providence, R.I., U.S.A.

(Received 26 September, 1978)

Abstract. The Luna-24 site is situated in Mare Crisium at a range of 18.4 km from Fahrenheit, an Eratosthenian-aged crater 6.4 km in diameter. Fahrenheit's ejecta deposits have been degraded to such an extent that secondary craters and rays cannot be unambiguously identified in the vicinity of the Luna-24 site. On the basis of an analogy between Fahrenheit and Lichtenberg B (a much younger crater of comparable size located in northern Oceanus Procellarum) Fahrenheit ejecta deposits near the sample site are inferred to have consisted of secondary crater clusters, subradially aligned secondary crater chains, and lineated terrain furrowed by fine-scale radial grooves. At the range of the Luna-24 site more than 80% of the mare surface should have been morphologically disturbed by the ballistic deposition of Fahrenheit ejecta. Blocks and fragment clusters of primary Fahrenheit ejecta ranging up to 5–20 m in diameter are inferred to have impacted the local surface at velocities of 165–230 m s^{-1} forming secondary craters ranging up to 100 m in diameter. The maximum depth of excavation of primary Fahrenheit ejecta deposited near the sample site is estimated to be at least 100 m. Primary Fahrenheit ejecta is expected to constitute a substantial fraction of the exterior deposits emplaced at the range of the Luna-24 site. Microgabbro and monomineralic fragments discovered in the Luna-24 drill core may have been derived from gabbroic rocks transported to the sample site by the Fahrenheit cratering event. This hypothesis is consistent with the widespread occurrence and characteristics of Fahrenheit ejecta anticipated in the vicinity of the Luna-24 site. Current interpretations of the drill core sample suggest that the Luna-24 regolith was deposited in its present configuration sometime during the last 0.3 AE implying that at least one local cratering event has occurred since the emplacement of Fahrenheit ejecta ~2.0 ± 0.5 AE ago.

1. Introduction

The Luna-24 mission to the southeast portion of Mare Crisium returned 170 g of lunar regolith obtained by drilling one to two metres into the mare surface. The sample site is situated in an area of mottled albedo approximately 35–50 km northwest of the highlands at the edge of the Crisium Basin. Holocrystalline gabbro and monomineralic fragments are the dominant lithologic type within the drill core, although basalt fragments, regolith breccia fragments, agglutinates, and glass spherules are also present (Barsukov, 1977; Florensky *et al.*, 1977). Highland rock types make up an extremely small fraction of the core sample (Bence and Grove, 1977).

Several investigators have suggested that the holocrystalline fragments found in the Luna-24 core may have been transported to the sample site by the Fahrenheit cratering event (Florensky *et al.*, 1977; Butler and Morrison, 1977; Basu *et al.*, 1978). The Luna-24 site is located 18.4 km east-southeast of the center of Fahrenheit, an Eratosthenian-aged crater with a rim crest diameter of 6.4 km. The average thickness of primary Fahrenheit ejecta deposited at the range of the sample site is estimated to be ~0.5–0.9 m (Butler

The Moon and the Planets **20** (1979) 281–300. 0165–0807/79/0203–0281$03.00

and Morrison, 1977; Ivanov and Comissarova, 1977). However at this range Fahrenheit's ejecta deposit is discontinuous and azimuthal variations in ejecta deposit thickness are large (Settle and Head, 1977). The probability of encountering primary Fahrenheit at the Luna-24 site cannot be estimated due to the degraded state of Fahrenheit's exterior deposits.

Without additional samples of Fahrenheit ejecta, and in the absence of high resolution photography and remote sensing measurements within southeastern Crisium, it is not possible to conclusively determine whether the gabbroic and monomineralic fragments in the Luna-24 soils were indeed excavated by Fahrenheit. However, the likelihood that these crystalline fragments constitute primary Fahrenheit ejecta can be assessed by considering the quantity, characteristics, and mode of deposition of Fahrenheit ejecta in the vicinity of the Luna-24 site. The purposes of this paper are to (1) estimate the depth of excavation of primary Fahrenheit ejecta transported to the range of the Luna-24 site, (2) assess the probability that primary Fahrenheit ejecta was actually deposited at the site, and (3) examine the manner in which this ejecta was emplaced.

2. Fahrenheit Crater: Structure and Morphology

The Fahrenheit cratering event excavated into basaltic mare deposits which fill the southeastern portion of the Crisium Basin. Boyce and Johnson (1977) have tentatively assigned ages of 3.4–3.7 AE to surface flow units occurring in the vicinity of Fahrenheit on the basis of size-frequency distributions of superimposed craters. Fahrenheit possesses a nearly circular rim crest, a reasonably symmetric cross-sectional geometry, and a small flat floor (see Figure 1). The crater formed in close proximity to a mare wrinkle ridge upon a gently sloping surface that rises to the southeast and east-northeast at angles of 2.9° and 2.3°, respectively (Lunar Topographic Orthophotomap 62B1).

The height of Fahrenheit's rim crest above the original ground surface varies from ~ 335 m (northeast rim) to ~225 m (southeast rim). Morphometric analysis of fresh lunar craters with diameter $D < 15$ km indicates that average crater rim height $H = 0.036D^{1.014}$ (Pike, 1977a). This relationship predicts an average rim height of 236 m for a crater 6.4 km in diameter in good agreement with measured values. The rim-to-floor depth of Fahrenheit varies from ~1420 m on the southwest side of the crater to ~1580 m on the southeast side; the average depth is ~1500 m. The average ratio of crater depth to diameter is 0.23 which is somewhat larger than the average depth/diameter ratio of 0.20 observed for fresh lunar craters 5–10 km in diameter (Pike, 1977a).

In sharp contrast to the fresh morphometric appearance of Fahrenheit, the exterior deposits surrounding the crater are substantially degraded (Figure 1). Copernican-aged craters comparable in size to Fahrenheit, such as Mösting C (Oberbeck *et al.*, 1974) and Lichtenberg B (Figure 2), are surrounded by continuous ejecta deposits that possess a hummocky and furrowed surface morphology, and contain ubiquitous dune-like features. Fahrenheit's continuous exterior deposits are characterized by subdued surface textures which can be faintly discerned in photographic transparencies. (Identification

Fig. 1. Southward looking view of the crater Fahrenheit (rim crest diameter = 6.4 km) situated in southeastern Mare Crisium (Apollo-17 panoramic camera frame 2223, Sun angle ~45°). Note the general lack of distinctive texturing within Fahrenheit's ejecta deposits. The Luna-24 site is adjacent to the upper left corner of the picture outside the field of view of the photograph.

of fine scale morphological patterns is partially hampered by the high sun illumination that exists in available high resolution photographs of Fahrenheit.) In addition, the area adjacent to Fahrenheit's rim crest is extensively pitted by smaller craters ($D < 500$ m) that postdate the formation of Fahrenheit.

Morphological studies of fresh lunar craters indicate that, on the average, the continuous deposits surrounding a crater with $D = 6.4$ km should extend to a range of 13–16 km, or ~4.5 crater radii (Oberbeck *et al.*, 1974; Moore *et al.*, 1974). The edge of Fahrenheit's continuous exterior deposits, however, is not clearly demarcated by variations in surface albedo or texture. Subtle variations in surface roughness may be correlated with the edge of Fahrenheit's continuous ejecta deposit, but it is difficult to develop an objective set of criteria to identify this morphological boundary on all sides of the crater (see Figure 1). Fahrenheit rays cannot be distinguished within the zone of discontinuous ejecta deposition, and any secondary crater chains or clusters formed by primary Fahrenheit ejecta have been modified to such an extent that they cannot be identified unambiguously.

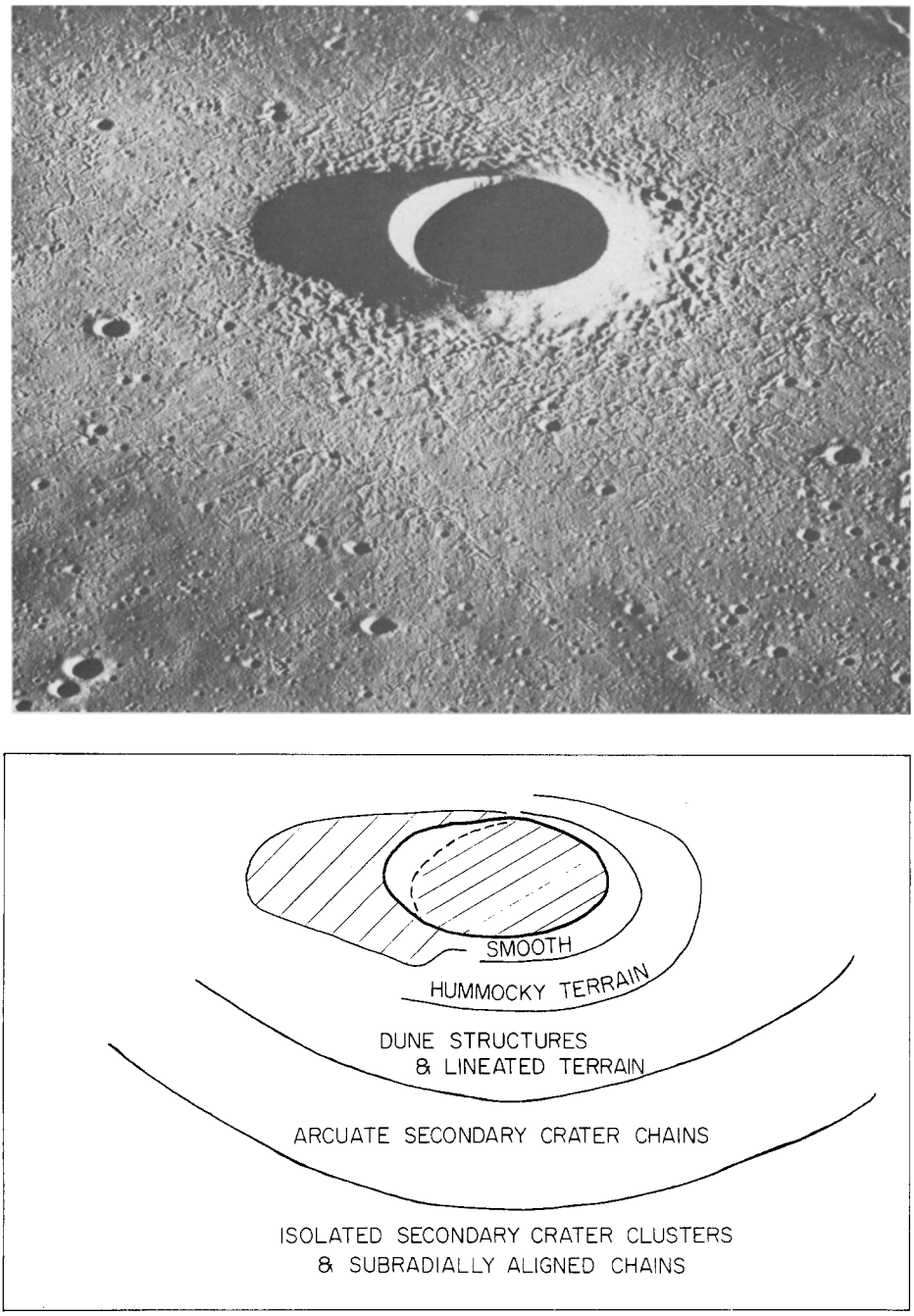

Fig. 2. Lichtenberg B is an extremely fresh-appearing Copernican-aged crater ($D = 4.9$ km) situated in northern Oceanus Procellarum (Apollo-15 panoramic camera frame 0363). Radial variations in the morphology of Lichtenberg B's ejecta deposits are schematically illustrated below the photograph (see text for detailed descriptions).

Morphological degradation of Fahrenheit's ejecta deposits is the result of long term exposure to impact bombardment processes which have reworked the near-surface portions of these deposits. The morphological freshness of a lunar impact crater is a function of its age and size. Smaller lunar craters possess relatively thinner ejecta deposits which are initially characterized by finer scale surface features. Small craters are consequently degraded at comparatively faster rates (Trask, 1971; Offield and Pohn, 1970; Swann and Reed, 1974; Neukum and König, 1976). Extensive morphological degradation is to be expected of Eratosthenian-aged craters the size of Fahrenheit, since regolith development and gardening will destroy the fine-scale textures of ejecta deposits associated with craters of this size without significantly altering crater morphometry (i.e., rim height and depth/diameter relationships).

Pohn and Offield (1970) have developed a morphological index scale which classifies the overall degradation state of a lunar crater on the basis of the morphology of its rim crest, walls, and exterior deposits. Within the Pohn and Offield classification scheme crater degradation states range from 0.0 (oldest) to 7.0 (youngest) and morphological variations have been explicitly described for three distinct crater size classes (Class I, $D > 45$ km; Class II, $D = 20$–45 km; Class III, $D = 8$–20 km). Fahrenheit closely resembles Rabbi Levi L (34.7°S, 23.1°E), an Eratosthenian-aged crater 12.6 km in diameter which has been rated at 5.5 on the Pohn and Offield scale of crater degradation (Pohn and Offield, 1970). Rabbi Levi L possesses a circular subdued rim crest, smooth interior walls, a flat floor, and remnant dune-like features within its exterior deposits (Lunar Orbiter IV frame 88H3). Offield and Pohn (1970) have demonstrated that the rate at which a crater's pristine morphology is subdued increases greatly for craters smaller than 8 km in diameter (Swann and Reed, 1974). Therefore, although the apparent degradation state of Fahrenheit would be rated at ~5.5 on the Pohn and Offield scale, its actual age of formation more closely corresponds to the absolute ages of larger craters with fresher morphological appearances.

Head (1975) has proposed an empirical correlation between the geological time scale and the Pohn and Offield spectrum of crater degradation states based upon estimates of the absolute ages of several large lunar craters. If Fahrenheit was slightly larger (i.e., large enough to belong to the Pohn and Offield Class III crater grouping), it would be somewhat better preserved and would probably be characterized by an apparent degradation state of ~5.6–5.9. This would correspond to an absolute age of ~2.0 ± 0.5 AE for the Fahrenheit cratering event (see Figure 3 in Head (1975)). Although crater age cannot be precisely determined by this morphological index technique, these relationships between crater size, morphology and degradation rates indicate that the state of degradation of Fahrenheit's deposits is not consistent with a formation age less than ~1.5 AE for Fahrenheit.

3. Depth of Excavation of Primary Fahrenheit Ejecta at the Luna-24 Site

Apparent crater dimensions are defined in this study as the dimensions of the observed crater measured at the elevation of the original (pre-existing) ground surface. The

apparent radius of Fahrenheit is 2630 m and its apparent depth is 1225 m. These are average values based upon four separate measurements on the northeast, southeast, southwest, and northwest sides of Fahrenheit. If we assume a parabolic form for the crater cavity (Dence, 1973), the volume of Fahrenheit below the original ground surface is 13.3km^3. Primary ejecta excavated by the Fahrenheit event accounts for the major portion of this volume. However, compression and structural uplift additionally account for a fraction of the apparent crater volume (Dence *et al.*, 1977).

The distribution of lunar crater ejecta has been investigated by examination of South Ray crater ejecta at the Apollo-16 site (Ulrich *et al.*, 1975), computer simulation of lunar cratering events (O'Keefe and Ahrens, 1976), and laboratory experiments conducted under terrestrial gravitational conditions (Stöffler *et al.*, 1975). These studies indicate that, to a first order approximation, the *average* thickness of *primary* ejecta deposited at range r on the lunar surface varies in proportion to $(r/R)^{-3}$, where R is the rim crest radius of a crater. McGetchin *et al.* (1973) have also employed a -3 radial decay relationship to describe radial variations in the thickness of basin ejecta deposits on the Moon. If primary crater ejecta is distributed in accordance with the -3 radial decay relation, then the total volume of primary ejecta equals $2\pi TR^2$, where T is the average rim thickness of primary ejecta (McGetchin *et al.*, 1973).

The average height of Fahrenheit's rim crest above the mare surface is ~270 m. On the basis of data from nuclear explosion craters Pike (1974) has proposed that structural uplift may account for ~30% of the rim height of large lunar craters. Adopting this proportion, the average rim thickness of primary Fahrenheit ejecta is estimated to be 190 m. The expression for total primary ejecta volume given above predicts that 12.2 km^3 of primary ejecta was transported beyond the rim of Fahrenheit. These estimates indicate that less than 10% of the volume of Fahrenheit crater below the original ground surface can be attributed to compression and structural uplift, which is generally consistent with measurements of ejecta and uplift volumes at Meteor Crater, Arizona (Roddy *et al.*, 1975).

An additional consequence of the -3 radial decay relation for primary ejecta distribution is that the volume of primary ejecta deposited beyond a given range r is equal to $(R/r)V_t$ where V_t is the total volume of primary ejecta (McGetchin *et al.*, 1973). Impact crater ejecta is excavated in such a manner that the shallowest material ejected from a transient cavity travels the greatest distances (Stöffler *et al.*, 1975). A *minimum* estimate of the maximum depth of excavation of primary Fahrenheit ejecta deposited in the vicinity of the Luna-24 site can be determined by assuming that the fraction of primary ejecta deposited at ranges beyond the Luna-24 site (~2.1 km^3) originated from a disk-shaped region situated within the uppermost portion of a parabolic excavation cavity. If the radius of the Fahrenheit excavation cavity was approximately equivalent to the presently observed apparent crater radius ($R_a = 2.63$ km), then the disk model described above indicates that primary Fahrenheit ejecta impacting in the vicinity of the Luna-24 site should have been excavated from depths of 100 m or less. This method of estimating the maximum depth of excavation of Fahrenheit ejecta arriving at the Luna-24 site does not take into consideration the relationship between ejecta particle

trajectories and the flow field established in the target material during a cratering event (Gault *et al.*, 1968). Ivanov and Comissarova (1977) have devised a heuristic model of impact crater excavation that accounts for particle motions during a cratering event, and have estimated a maximum depth of excavation of ~400 m for Fahrenheit ejecta at the Luna-24 site. The range of 100–400 m probably brackets the maximum depth of excavation of primary Fahrenheit ejecta actually deposited near the Luna-24 site.

Spectral reflectance data reported by Head *et al.* (1978) indicate that the Luna-24 site is situated in a mare unit characterized by a relatively low titanium oxide content (TiO_2 less than ~2%). This unit is regionally overlain by a thin, discontinuous unit possessing a comparatively higher albedo and higher titanium content that occurs in the immediate vicinity of Fahrenheit. Mare material excavated from depths of 100–400 m by the Fahrenheit cratering event is expected to be derived from the same stratigraphically lower, low titanium unit which is exposed at the Luna-24 site. Therefore, the chemical composition of local surficial material and primary Fahrenheit ejecta at the Luna-24 site could be quite similar.

5. Mode of Emplacement of Primary Fahrenheit Ejecta at the Luna-24 Site

5.1. *Analogy between Fahrenheit and Lichtenberg B*

The original morphology of Fahrenheit's ejecta deposits in the vicinity of the Luna-24 site can be inferred by examining a fresh crater of comparable site that has formed in a similar type of target material. Lichtenberg B is a Copernican-aged crater in northern Oceanus Procellarum (33.25° N, 61.5° W) with a rim crest diameter of 4.9 km. Lichtenberg B excavated into one of the youngest lava flows on the lunar surface (Whitaker, 1972; Whitford-Stark and Head, 1978); this flow unit has been assigned an age of 2.6 ± 0.3 AE by Boyce (1976) on the basis of superimposed crater density.

Lichtenberg B possesses a sharply-defined, circular rim crest and smooth interior walls. Its exterior deposits are characterized by a variety of fine-scale surface textures (Figure 2). The state of degradation of Lichtenberg B would be rated at 6.5 ± 0.2 on the Pohn and Offield scale. As discussed above, smaller craters experience the greatest rates of morphological degradation, particularly craters less than 8 km in diameter (Offield and Pohn, 1970). The small size and extremely fresh appearance of Lichtenberg B indicate that it is a very young crater. On the basis of the empirical correlation between Pohn and Offield degradation states and the geological time scale proposed by Head (1975), Lichtenberg B is inferred to be no more than 0.5 AE old.

Both Fahrenheit and Lichtenberg B formed in mare flow units which had been exposed to impact gardening processes for a significant period of time. In the case of Fahrenheit, the period between flow emplacement and crater excavation was ~1.5 AE (~3.5–2.0 AE before present), whereas for Lichtenberg B this time period was on the order of 2.0 AE (~2.6–0.5 AE before present). Regolith thicknesses encountered by the two cratering events should have been comparable since the shorter period available for regolith development prior to the Fahrenheit event is partially compensated by the higher flux

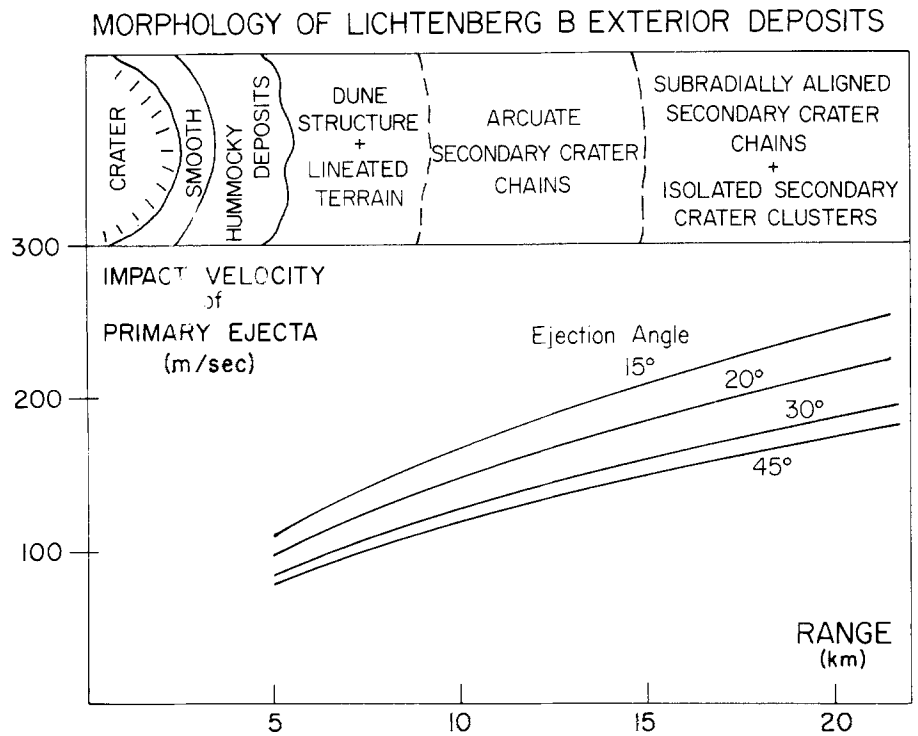

Fig. 3. With increasing range from Lichtenberg B, primary ejecta impacts the local mare surface at progressively greater velocities. The degree to which primary Lichtenberg B ejecta excavates and mixes with local regolith material is reflected in the morphology of the ejecta deposit emplaced at different ranges. Ejecta emplacement conditions at a range of 18 km should generally correspond to the manner in which primary Fahrenheit ejecta was emplaced near the Luna-24 site.

of impacting projectiles during earlier geological epochs (Quaide and Oberbeck, 1975). The structure of the target medium in which both Fahrenheit and Lichtenberg B formed would thus have consisted of a relatively incompetent regolith layer several meters thick overlying a more competent but fractured substrate composed of multiple lava flow units. Therefore, primary ejecta excavated by Fahrenheit and Lichtenberg B impacted mare surfaces with essentially the same gross structure and physical properties. In addition, primary ejecta excavated by the two cratering events should have impacted the mare surface at approximately equivalent velocities at any given range due to the size similarity between Fahrenheit and Lichtenberg B. These considerations indicate that Fahrenheit and Lichtenberg B ejecta were ballistically deposited in a closely corresponding fashion and imply that the fine scale surface textures presently observed within Lichtenberg B's exterior deposits should be analogous to the pristine morphology of the ejecta deposits surrounding Fahrenheit.

Radial variations in the morphology of Lichtenberg B's exterior deposits are indicative of increasing interaction between primary ejecta and the pre-existing ground surface with increasing range (Figures 2 and 3). The rim deposits of Lichtenberg B possess a

smooth surface morphology from the crater's rim crest to a range of ~1.4R (measured from the crater's center). At this range the continuous ejecta deposit develops a hummocky surface texture consisting of low hills and gently dipping topographic swales. With increasing range adjacent hills and depressions become more tightly spaced and the hummocky surface texture develops a much more rugged topographic expression. At a range of ~2.2R hummocky terrain grades into a series of arcuate ridges commonly associated with adjacent downrange troughs. Similar features have been observed within the continuous exterior deposits of Mösting C and Linné (Oberbeck *et al.*, 1974; Morrison and Oberbeck, 1975). These arcuate, dune-like structures are separated by relatively flat areas which are furrowed by fine scale radial and subradial grooves, indicating substantial interaction between Lichtenberg B ejecta and pre-existing terrain. Non-lineated interdune ground is rarely observed.

Dune structures grade into arcuate secondary crater chains with scalloped outlines at ranges of ~3.7R. Radially lineated terrain is commonly observed in association with these arcuate crater chains. At a range of ~6R arcuate crater chains begin to break up into clusters of individual secondary craters and subradially aligned, linear crater chains. Lineated terrain frequently occurs downrange of subradially aligned crater chains; however, isolated patches of radially grooved terrain are not uncommon beyond a range of 6R. Significant areas of unaffected, pre-existing terrain are initially encountered at ranges of 5R–6R. A well-developed ray pattern surrounds Lichtenberg B and extends beyond a range of 10R.

5.2. *Morphology and Occurrence of Fahrenheit Deposits at Sample Site*

The mode of deposition of primary Fahrenheit ejecta in the vicinity of the Luna-24 site can be inferred by examining secondary cratering effects at comparable ranges from Lichtenberg B. Primary Fahrenheit ejecta was deposited near the Luna-24 site at impact velocities of 165–230 m s^{-1}, assuming a range of particle ejection angles of 45°–15°, respectively (see Equation A7 of Oberbeck *et al.* (1975); angles measured from horizontal). If ejection angles of Fahrenheit and Lichtenberg B ejecta were generally similar, Lichtenberg B ejecta would have been deposited at impact velocities of 165–230 m s^{-1} at a range of ~18 km from the crater center (Figure 3). At this range Lichtenberg B's ejecta deposits principally consist of subradially aligned secondary crater chains, and lineated terrain furrowed by fine-scale radial grooves. Isolated secondary craters and secondary crater clusters also occur at this range. Patches of unaffected, pre-existing terrain represent ~20% of the area encountered at a range of 18 km from the center of Lichtenberg B. The amount of ejecta deposited at a particular *absolute* range (e.g., r = 18 km) from a crater increases, on the average, with increasing crater size (McGetchin *et al.*, 1973; Figure 10 in Morrison and Oberbeck (1975)). Therefore, since Fahrenheit is somewhat larger than Lichtenberg B, the frequency of occurrence of unaffected, pre-existing terrain at a range of 18 km from Fahrenheit should be less than ~20%. If the analogy between these two craters is accurate, the probability that the Luna 24 site is situated within an area affected by the ballistic deposition of Fahreheit ejecta is greater than 80%.

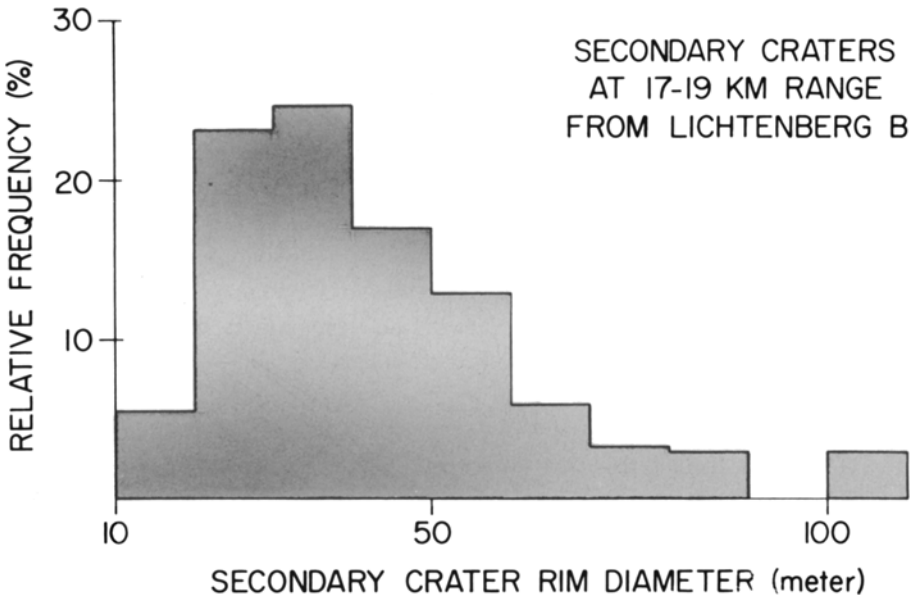

Fig. 4. Relative frequency distribution of Lichtenberg B secondary craters observed at ranges of 17–19 km (Apollo-15 panoramic camera frames 0362 and 0363). This relative size frequency distribution is based upon a total sampling of 271 craters mapped over a 90° sector of Lichtenberg B's discontinuous ejecta deposit. Several considerations suggest that this distribution may underrepresent the relative abundance of smaller secondary craters ($D < 25$ m) and larger isolated secondary craters ($D > 70$–80 m) situated at these ranges.

5.3. *Primary Ejecta Block Size*

Figure 4 displays the relative size frequency distribution of secondary craters observed at ranges of 17–19 km from the center of Lichtenberg B. At these ranges secondary craters are generally 10–100 m in diameter; craters with diameters of 20–60 m are particularly abundant. The crater size distribution presented in Figure 4 is based upon a sample of 271 secondary craters mapped over a 90° sector of Lichtenberg B's discontinuous ejecta deposit. Identification of secondary craters with diameters less than ~25 m was complicated by variations in contrast and solar illumination within available photographs. Craters less than 10 m in diameter could not be distinguished due to photographic resolution limitations. For these reasons it is likely that the relative frequency of secondary craters formed at these ranges actually increases with decreasing crater size ($D < 30$ m), contrary to the data trend shown in Figure 4. It was also difficult to unambiguously identify isolated Lichtenberg B secondaries which were not associated with crater chains, high albedo ray patches, or radially grooved terrain. If the largest Lichtenberg B secondary craters are preferentially formed or better preserved in areas which have not been affected by ray deposition or radial furrowing, then the frequency distribution shown in Figure 4 may underrepresent the relative abundance of large Lichtenberg B secondaries ($D > 70$–80 m) occurring at ranges of 17–19 km.

Variations in secondary crater size reflect differences in the size, structure and impact velocity of primary ejecta fragments, as well as local variations in target (regolith and mare) properties. Several investigators have developed generalized scaling relationships which relate impact crater size to projectile kinetic energy. These scaling relationships can be applied to individual Lichtenberg B secondary craters in order to estimate the size of the primary ejecta fragments that formed these craters.

On the basis of explosion cratering experiments Oberbeck *et al.* (1975), have proposed that impact crater diameter (D) varies as a function of projectile kinetic energy (E) in such a manner that $D \propto E^{1./3.4}$. Oberbeck *et al.* (1975) devised a proportionality constant between D and E appropriate to lunar cratering events by applying a gravity correction factor to data obtained from two shallow burial, nuclear cratering experiments (nominal yield equal to 5×10^{19} erg). Their model scaling relationship indicates that:

$$D = 2. \times 10^{-7} E^{0.294}, \tag{1}$$

where D is crater rim diameter in km and E is in erg. Moore (1976) has presented an empirical scaling relationship based upon terrestrial missile impact experiments performed in a variety of naturally occurring target materials (e.g., sand, alluvium, soil, and rock), in which:

$$V_a = 10^{-11.433} E^{1.205}, \tag{2}$$

where V_a is apparent crater volume (cm^3) measured below the original ground surface. Moore's experiments encompass a range of projectile kinetic energy of 10^{14}–10^{16} erg, and in the majority of these experiments projectile impact velocity (typically on the order of several hundred meters per second; Moore, pers. comm.) was considerably greater than the acoustic velocity of the target media. Culp and Hooper (1961) have conducted laboratory scale cratering experiments in which twenty-two caliber (lead) rifle bullets impacted into sand at velocities of 70–500 $m\,s^{-1}$. The acoustic velocity of sand is on the order of 100 $m\,s^{-1}$ and, therefore, this experimental test series spanned a range of cratering regimes from low velocity impacts to hypervelocity cratering events. The results of these experiments indicate that

$$V_a = 9.23 \times 10^{-3} m_p v_p^{1.452}, \tag{3}$$

where m_p is projectile mass in grams, v_p is projectile velocity in $m\,s^{-1}$, and V_a is in cm^3. Equation (3) represents a least squares fit to data presented graphically in Figure 4 of Culp and Hooper (1961); the fitting procedure employed 31 data points and achieved a correlation coefficient of 0.99. These laboratory experiments were performed under terrestrial gravitational conditions and encompassed a range of projectile kinetic energy of 10^{8}–10^{11} erg.

Impact crater size depends in part upon the strength of the gravity field in which the crater forms (Gault and Wedekind, 1977). Therefore, in order to apply Equations (2) and (3) to Lichtenberg B secondary craters, it is necessary to account for differences between gravitational conditions on the Earth and the Moon. The interior shape of

small non-terraced craters can be generally represented by a parabolic surface (Dence, 1973), in which case the volume of a crater below the original ground surface (V_a) is given by

$$V_a = \frac{\pi}{8} d_a D_a^2, \tag{4}$$

where d_a and D_a are the depth and diameter of the apparent crater. Equation (4) can be rewritten as

$$V_a = \frac{\pi}{8} k D_a^3, \tag{5}$$

where k is the depth/diameter ratio of the apparent crater (d_a/D_a). If two projectiles with equivalent kinetic energies impacted the Moon and the Earth, the ratio of crater volume on the two planetary surfaces would be

$$\frac{V_a\,(\text{Moon})}{V_a(\text{Earth})} = \frac{\pi k_m D_{am}^3/8}{\pi k_e D_{ae}^3/8} = \frac{k_m}{k_e}\left(\frac{D_{am}}{D_{ae}}\right)^3. \tag{6}$$

Gault and Wedekind (1977) have experimentally demonstrated that over a wide range of gravitational acceleration the ratio of depth to diameter (k) and the ratio of apparent crater diameter to rim crest diameter (D_a/D) are essentially constant. Therefore Equation (6) can be simplified to

$$\frac{V_a\,(\text{Moon})}{V_a\,(\text{Earth})} = \left(\frac{D_m}{D_e}\right)^3, \tag{7}$$

where D is crater rim crest diameter.

In the absence of material strength effects crater diameter would vary in proportion to gravity (g) in such a manner that $D \propto g^{-0.25}$ (Gault and Wedekind, 1977). However the finite strength of geological materials serves to decrease the absolute value of the exponent in this gravity scaling relationship. Experimentally determined values of the exponent range from −0.165 for dry quartz sand to −0.08 for moist (cohesive) sand (Gault and Wedekind, 1977; Viktorov and Stepenov, 1960). Assuming that $D \propto g^{-0.1}$ for cratering in regolith and fractured mare materials, the crater volume ratio becomes

$$\frac{V_a\,(\text{Moon})}{V_a\,(\text{Earth})} = \left(\left(\frac{g_m}{g_e}\right)^{-0.1}\right)^3 = \left(\frac{g_m}{g_e}\right)^{-0.3} = 1.7165. \tag{8}$$

This factor represents the difference in apparent crater volume that would be produced by equivalent projectile impacts on the Moon and Earth. Empirical relationships between crater volume and projectile energy should be adjusted accordingly in order to be applicable to lunar conditions. For the case of lunar cratering events Equation (2) becomes

$$V_a = 6.334 \times 10^{-12} E^{1.205}, \tag{9}$$

and Equation (3) becomes

$$V_a = 1.585 \times 10^{-2} m_p v_p^{1.452} . \quad (10)$$

Given the size of a Lichtenberg B secondary crater and the impact velocity of the projectile that formed the crater, Equations (1), (9), and (10) provide independent estimates of projectile diameter. The impact velocity of primary Lichtenberg B ejecta can be determined by assuming a ballistic particle trajectory (Equation (A7) of Oberbeck *et al.* (1975)) and an average particle ejection angle of 30° (ballistic range is measured from $R/2$ where R is rim crest crater radius). Apparent crater volume (V_a) is calculated by assuming: (a) parabolic crater shape, (b) apparent crater diameter/rim crest diameter = 0.83 (Pike (1977b), pers. comm.), and (c) apparent crater depth/rim crest diameter = 0.09 for secondary craters (Pike, pers. comm.; Pike, 1976; Pike and Wilhelms, 1978). Primary Lichtenberg B ejecta is assumed to consist of coherent, spherical blocks of basalt with a density of 2.8 gm cm^{-3}. Note that block size estimates are not greatly affected by changes in crater morphometry assumptions due to the cube root dependence of block size on inferred projectile mass.

This method of estimating projectile size was applied to the sample of Lichtenberg B secondary craters observed at ranges of 17–19 km (Figure 4). Primary ejecta block size distributions inferred by the three scaling relationships are presented in Figure 5. The frequency distributions in Figure 5 differ substantially and principally reflect the cratering efficiency of the various projectiles and explosives employed in the experiments described above. For example, Culp and Hooper (1961) used solid projectiles of high density material (lead bullets) which excavated and displaced comparatively large volumes of target material per unit projectile mass. Thus the block sizes inferred by the Culp and Hooper scaling relation (Equation (10)) are relatively small (1–10 m). The missiles employed in Moore's (1976) experiments were not solid throughout and consequently these projectiles were less efficient excavators. The model proposed by Oberbeck *et al.* (1975) implicitly assumes that the amount of energy partitioned into cavity formation by nuclear explosion and impact cratering events is the same. Nuclear cratering events release large quantities of energy as waste heat and radiation and are significantly less efficient at cavity excavation compared to the lead projectiles employed in Culp and Hooper's experiments. As a result, block sizes determined by the Oberbeck *et al.* (1975) scaling relationship (Equation (1)) are significantly larger than size estimates inferred by the other two scaling relations (Figure 5).

Coherent blocks of basalt impacting at velocities of 165–230 m s^{-1} would probably be more efficient excavators than nuclear explosive devices of comparable energy but would also produce a smaller crater volume per unit projectile mass than solid lead projectiles. Therefore it is reasonable to expect that the majority of the secondary craters observed at ranges of 17–19 km from Lichtenberg B were produced by blocks of primary ejecta with diameters on the order of 5–20 m (Figure 5). If primary ejecta were deposited as clusters of fragments rather than coherent blocks (Oberbeck *et al.*, 1975), the largest fragment clusters arriving at these ranges would have been greater than ~10–20 m in diameter.

The structure of the relative frequency distributions presented in Figure 5 may be some-

what misleading. As discussed previously, the empirical size distribution of Lichtenberg B secondary craters (Figure 4) may under-represent the relative abundance of craters with $D < 25$ m at these ranges. Therefore it is probable that primary ejecta blocks less than 2–5 m in diameter are much more abundant at ranges of 17–19 km than indicated in Figure 5.

5.4. *Post-Deposition State of Primary Ejecta*

Primary Lichtenberg B ejecta deposited at a range of 18 km is inferred to have impacted the mare surface at velocities of 165–230 m s^{-1}. In situ measurements of the compressional

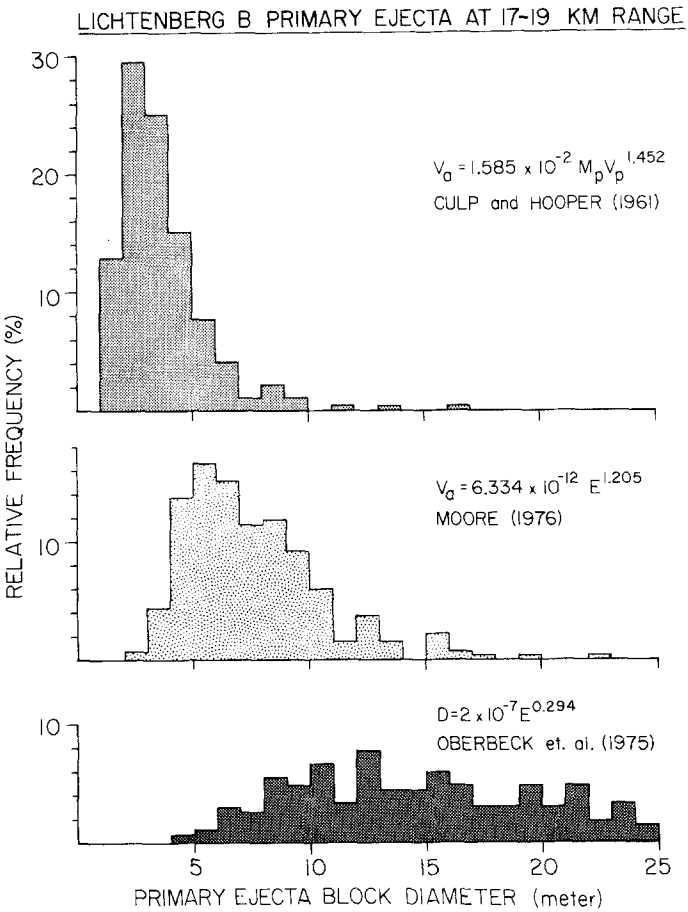

Fig. 5. Relative block size distributions of primary Lichtenberg B ejecta particles forming the secondary craters observed at ranges of 17–19 km (Figure 4). Block sizes have been estimated employing scaling relations which express crater size as a function of projectile energy, assuming that primary ejecta projectiles are coherent spheres of basalt. If primary ejecta consists of clusters of fragments, then the diameter of fragment clusters would be even greater than the block diameters presented in this figure.

wave velocity of mare regolith at the Apollo landing sites indicate that the acoustic velocity of mare soils is consistently on the order of $100\,m\,s^{-1}$ (Nakamura *et al.*, 1975). Therefore, secondary cratering events associated with ballistic deposition of Lichtenberg B ejecta at this range would not necessarily be equivalent to hypervelocity cratering events in which projectile velocities commonly exceed target acoustic velocities by a factor of 5 or more.

Oberbeck *et al.* (1975) have employed the scaling relation described above (Equation (1)) to estimate the amount of secondary crater ejecta excavated by a particular primary ejecta block or fragment cluster. For an average ejection angle of 30° the model of Oberbeck *et al.* (1975) predicts that primary ejecta projectiles impacting at a range of 18 km from Lichtenberg B excavated 1.5–0.6 times their own mass in the process of forming secondary craters 10–100 m in diameter. It is difficult to envision an impact cratering process in which a projectile excavates less than its own mass, since it intuitively seems that under these conditions more material is locally being 'deposited' than is being excavated. However this apparent paradox may be partially explained by: (a) density differences between projectile and target materials (e.g., density ratio of coherent basalt/near-surface regolith $\sim 2.8/1.8 = 1.6$), (b) target compression in relatively porous regolith material (Stöffler *et al.*, 1974, 1975), and (c) ejection of the major portion of a primary ejecta projectile during secondary crater formation. The numerical results of the Oberbeck *et al.* model qualitatively indicate that Lichtenberg B deposits emplaced at a range of 18 km should, *on the average*, contain a substantial fraction of primary Lichtenberg B ejecta.

Culp and Hooper's (1961) laboratory experiments demonstrate that projectile deformation is relatively limited at impact velocities less than $245\,m\,s^{-1}$ in the case of metallic projectiles striking sand targets. Larger scale missile impact experiments reported by Moore (1976) similarly indicate that at velocities less than $250\,m\,s^{-1}$ missile projectiles are not extensively fragmented and the major portion of the impacting projectile remains unburied after the cratering event (see Figure 39 in Moore (1976)). Although Lichtenberg B ejecta particles may not have been as competent as the projectiles employed in these experiments, these results suggest that primary Lichtenberg B ejecta deposited at a range of 18 km was not intensely comminuted upon impact. At impact velocities of $165–230\,m\,s^{-1}$ primary ejecta particles should have been ruptured and brecciated in the process of excavating local material. Shock metamorphic effects produced by such low velocity impacts would have been minor.

5.5. *Summary*

The process of ejecta emplacement at ranges of 17–19 km from Lichtenberg B should have generally corresponded to the manner in which Fahrenheit ejecta was deposited near the Luna-24 site. However the two ejecta emplacement processes may not have been exactly equivalent due to such factors as: (a) azimuthal variations in ejecta distribution (Lichtenberg B ejecta deposits are symmetrically distributed but the symmetry of Fahrenheit's ejecta deposits cannot be precisely determined), and (b) differences in

mare target characteristics (primary ejecta block size distributions are partially determined by fracture spacings in target materials; fracture systems within the Lichtenberg B and Fahrenheit target materials may have been different). Nevertheless, in the absence of detailed information about the structure and morphology of Fahrenheit's ejecta deposits, the analogy between the two craters provides the best means of inferring the characteristics of primary Fahrenheit ejecta deposited near the Luna-24 site.

On the basis of this analogy, the ballistic emplacement of Fahrenheit ejecta in the vicinity of the sample site is characterized as follows. Primary Fahrenheit ejecta deposited near the Luna-24 site consisted of blocks and fragment clusters ranging up to 5–20 m in diameter. These primary ejecta particles impacted the regolith surface at velocities of 165–230 m s^{-1} and excavated 0.6–1.5 times their own mass, forming secondary craters ranging up to 100 m in diameter. Secondary craters 20 m–60 m in diameter were particularly abundant in the immediate vicinity of the Luna-24 site. Deposition of primary ejecta blocks greater than 2 m in diameter was accompanied by widespread ballistic sedimentation of smaller sized ejecta particles responsible for the production of rays and radially grooved terrain. Primary ejecta particles were primarily ruptured upon impact and were not intensely comminuted. A major fraction of these primary ejecta fragments subsequently remained on or near the local regolith surface.

6. Provenance of Holocrystalline Fragments in the Luna 24 Core Sample

Gabbro fragments within the Luna 24 core possess an equigranular texture with mineral grain size ranging from 0.1 mm to 0.5–0.7 mm (Florensky *et al.*, 1977). Detailed petrographic and petrologic studies indicate that the gabbro and monomineralic fragments were derived from gabbroic rocks with a grain size greater than 1 mm (Grove and Bence, 1977). These source rocks presumably crystallized in a subsurface environment characterized by relatively slow cooling rates (Basu *et al.*, 1978). For purposes of comparison, crystalline 'gabbroic' material nearly devoid of interstitial glass has been observed at depths of 50–60 m within a prehistoric lava lake in Hawaii (Moore and Evans, 1967). The grain size of plagioclase and clinopyroxene crystals within these terrestrial lava lake samples is comparable to the grain size of the Luna-24 gabbros, although the petrographic fabric and chemical composition of the two rock types is distinctly different (Moore and Evans, 1967; Tarasov *et al.*, 1977). The actual depth of formation of fine-grained gabbroic rock units within the Crisium Basin is not rigorously constrained by currently available petrologic analyses of the Luna-24 samples.

Gabbroic rocks situated at a significant depth below the mare surface may have been excavated and incorporated into surficial soils by an impact cratering event. Alternatively, gabbro blocks may have been entrained in flowing magma at depth and transported to the surface as xenoliths. If a gabbro lens or layer is situated at a depth of 25–30 m in the immediate vicinity of the sample site, then gabbroic fragments may have been initially incorporated into the surface regolith by one or more local craters 150–200 m in diameter (Florensky *et al.*, 1977; Butler and Morrison, 1977; crater morphometric relations as

given by Pike, 1977b). However, if the Luna-24 crystalline fragments were derived from a gabbro lens that formed at depths of 50 m or greater, they could not have been excavated from their original position by any of the craters in the immediate vicinity of the sample site. Under these circumstances Fahrenheit is a likely source of the gabbroic fragments because of its size (6.4 km diameter), proximity (18.4 km range), and relatively young Eratosthenian age.

On the basis of an analogy between Fahrenheit and Lichtenberg B (a much younger crater of comparable size) this study has shown that there is a high probability ($> 80\%$) that the Luna-24 site was morphologically disturbed by the deposition of Fahrenheit ejecta. At this range primary Fahrenheit ejecta is inferred to have consisted of blocks and fragment clusters ranging up to 5–20 m in diameter. The maximum depth of excavation of these primary ejecta particles was at least 100 m and may have been as great as 400 m. Primary Fahrenheit ejecta would have a basaltic chemical composition and should not have been shock metamorphosed to any significant degree. Fahrenheit ejecta particles impacted the local surface at velocities of 165–230 m s^{-1} and were brecciated in the process of excavating local regolith material. A substantial fraction of primary Fahrenheit ejecta deposited near the site would have subsequently remained on or near the regolith surface.

The relative abundance, gabbroic composition, and unshocked character of the holocrystalline fragments discovered in the Luna-24 core sample are consistent with the widespread occurrence of Fahrenheit deposits and the characteristics of primary Fahrenheit ejecta anticipated at the range of the Luna-24 site. Although these gabbroic fragments cannot be unambiguously identified as primary Fahrenheit ejecta, the evidence presented here demonstrates that this interpretation is in agreement with the inferred mode of deposition of Fahrenheit ejecta at the sample site. If subsequent petrologic analysis and experimentation indicates that the Luna-24 gabbroic fragments originally crystallized at depths of 50 m or greater, then the probability that these fragments are primary Fahrenheit ejecta would be increased.

Variations in particle size, agglutinate content, cosmic ray and solar flare irradiation, and neutron fluence observed within the Luna-24 core do not conform to the variations in these parameters which would naturally occur as a function of depth due to long term bombardment and irradiation processes. The complex structure of the core sample suggests that the upper few meters of regolith at the Luna-24 site consists of a mixture of soils with distinctive size characteristics, surface maturities and irradiation histories (Bogard and Hirsch, 1978; McKay *et al.*, 1978; Morris, 1978; Wasserburg *et al.*, 1978). On the basis of cosmogenic noble gas concentrations and surface maturity indices, and in consideration of the other factors cited above, Bogard and Hirsch (1978) have tentatively concluded that the Luna-24 regolith was deposited over a relatively short period sometime during the past 0.3 AE.

The state of degradation of Fahrenheit and its exterior deposits indicates that the Fahrenheit cratering event occurred more than 1.5 AE ago. Therefore the regolith structure observed within the Luna-24 drill core was not produced by the ballistic deposition

of Fahrenheit ejecta at the sample site. The crystalline fragments within the core sample generally possess angular shapes, fresh fracture surfaces, and lack microcraters and surface melt features (Florensky *et al.*, 1977). Although these morphological features may partly be due to core drilling operations, they suggest that the crystalline fragments have not been exposed to near-surface impact weathering phenomena for substantial periods of time. The majority of these fragments may have been formed during the most recent cratering episode (<0.3 AE) by brecciation of larger gabbroic rocks (primary Fahrenheit ejecta?) that were locally present within the mare regolith.

Acknowledgements

The authors wish to thank Fred Hörz and Peter Schultz for thoughtful reviews of an earlier version of this paper and D. Bogard, W. Hirsch, and R. Morris for sharing preprints of their Luna-24 papers. Selenographic coordinates of Lichtenberg B secondary craters were determined directly from Apollo-15 panoramic frames 362 and 363 using a computer program originally developed by Ken Jones which was modified by Ed Robinson for the purposes of this study. The effort and patience of Sally Bosworth and Laurie Raymond in preparing the manuscript for publication is sincerely appreciated. We gratefully acknowledge the assistance of the National Space Science Data Center which provided the Apollo-15 and -17 panoramic photography used in this study and the support of NASA Grant NGR 40-002-116.

References

Barsukov, V. L.: 1977, 'Preliminary Data for the Regolith Core Brought to Earth by the Automatic Lunar Station Luna 24', *Proc. 8th Lunar Sci. Conf.*, pp. 3303–3318.

Basu, A., McKay, D. S., and Fruland, R. M.: 1978, 'Petrography, Mineralogy and Source Rocks of Luna 24 Drill Core Soils', in *Mare Crisium: The View from Luna 24*, Pergamon Press, New York, pp. 321–338.

Bence, A. E. and Grove, T. L.: 1977, 'The Highland Component in the Luna 24 Core' (abs.), Conference on Luna 24, Lunar and Planetary Institute, Houston, Tex, pp. 22–24.

Bogard, D. D. and Hirsch, W. C.: 1978, 'Noble Gases in Luna 24 Core Soils', in *Mare Crisium: The View from Luna 24*, Pergamon Press, New York, pp. 105–116.

Boyce, J. M.: 1976, 'Ages of Flow Units in the Lunar Nearside Maria Based on Lunar Orbiter IV Photographs', *Proc. 7th Lunar Sci. Conf.*, pp. 2717–2728.

Boyce, J. M. and Johnson, D. A.: 1977, 'Age of Flow Units in Mare Crisium Based on Crater Density', *Proc. 8th Lunar Sci. Conf.*, pp. 3495–3502.

Butler, P. and Morrison, D. A.: 1977, 'Geology of the Luna 24 Landing Site', *Proc. 8th Lunar Science Conf.*, pp. 3281–3301.

Culp, F. L. and Hooper, H. L.: 1961, 'Study of Impact Cratering in Sand', *J. Appl. Phys.* **32**, 2488–2484.

Dence, M. R.: 1973, 'Dimensional Analysis of Impact Structures', *Meteoritics* 8, 343–344.

Dence, M. R., Grieve, R. A. F., and Robertson, P. B.: 1977, 'Terrestrial Impact Structures: Principal Characteristics and Energy Considerations', in D. J. Roddy, R. O. Pepin, and R. B. Merrill (eds.), *Impact and Explosion Cratering*, Pergamon Press, New York, pp. 247–275.

Florensky, C. P., Basilevsky, A. T., Ivanov, A. V., Pronin, A. A., Rode, O. D.: 1977, 'Luna 24: Geologic Settling of Landing Site and Characteristics of Sample Core' (Preliminary Data), *Proc. 8th Lunar Sci. Conf.*, pp. 3257–3279.

Gault, D. E., Quaide, W. L., and Oberbeck, V. R.: 1968, 'Impact Cratering Mechanics and Structures', in B. M. French and N. M. Short (eds.), *Shock Metamorphism of Natural Materials*, Mono Book Corp., Baltimore, Md., pp. 87–99.

Gault, D. E. and Wedekind, J. A.: 1977, 'Experimental Hypervelocity Impact into Quartz Sand – II, Effects of Gravitational Acceleration', in D. J. Roddy, R. O. Pepin, and R. B. Merrill (eds.), *Impact and Explosion Cratering*, Pergamon Press, New York, pp. 1231–1244.

Grove, T. L. and Bence, A. E.: 1977, 'Petrogenesis of Gabbros from Mare Crisium' (abs.), Conference on Luna 24, Lunar and Planetary Institute, Houston, Tex., pp. 64–67.

Head, J. W.: 1975, 'Processes of Lunar Crater Degradation: Changes in Style with Geologic Time', *The Moon* **12**, 299–329.

Head, J. W., Adams, J. B., McCord, T. B., Pieters, C., and Zisk, S.: 1978, 'Regional Stratigraphy and Geologic History of Mare Crisium', in *Mare Crisium: The View from Luna 24*, Pergamon Press, New York, pp. 43–74.

Ivanov, B. A. and Comissarova, L. I.: 1977, 'The Simple Hydrodynamic Model of Cratering' (abs.), *Lunar Science VIII*, Lunar and Planetary Institute, Houston, Tex., pp. 499–501.

McGetchin, T. R., Settle, M., and Head, J. W.: 1973, 'Radial Thickness Variation in Impact Crater Ejecta: Implications for Lunar Basin Deposits', *Earth Planet. Sci. Letters* **20**, 226–236.

McKay, D. S., Basu, A., and Waits, G.: 1978, 'Grain Size and Evolution of Luna 24 Soils', in *Mare Crisium: The View from Luna 24*, Pergamon Press, New York, pp. 125–136.

Moore, H. J.: 1976, 'Missle Impact Craters (White Sands Missle Range, New Mexico) and Applications to Lunar Research', U.S. Geological Survey Prof. Paper 812-B, p. B1-47.

Moore, H. J., Hodges, C. A., and Scott, D. H.: 1974, 'Multiringed Basins – Illustrated by Orientale and Associated Features', *Proc. 5th Lunar Sci. Conf.*, pp. 71–100.

Moore, J. G. and Evans, B. W.: 1967, 'The Role of Olivine in the Crystallization of the Prehistoric Makaopuhi Tholeiitic Lava Lake, Hawaii', *Contrib. Mineral. Petrol.*, **15**, 202–223.

Morris, R. V.: 1978, 'FMR and Magnetic Studies of Luna 24 Soils and > 1 mm Soil Particles', in *Mare Crisium: The View from Luna 24*, Pergamon Press, New York, pp. 117–124.

Morrison, R. H. and Oberbeck, V. R.: 1975, 'Geomorphology of Crater and Basin Deposits – Emplacement of the Fra Mauro Formation', *Proc. 6th Lunar Sci. Conf.*, pp. 2503–2530.

Nakamura, Y., Dorman, J., Duennebier, F., Lammlein, D., and Latham, G.: 1975, 'Shallow Lunar Structure Determined from the Passive Seismic Experiment', *The Moon*, **13**, 57–66.

Neukum, G. and König, B.: 1976, 'Dating of Individual Lunar Craters', *Proc. 7th Lunar Sci. Conf.*, pp. 2867–2881.

Oberbeck, V. R., Morrison, R. H., Hörz, F., Quaide, W. L., Gault, D. E.: 1974, 'Smooth Plains and Continuous Deposits of Craters and Basins', *Proc. 5th Lunar Sci. Conf.*, pp. 111–136.

Oberbeck, V. R., Hörz, F., Morrison, R. H., Quaide, W. L., and Gault, D. E.: 1975, 'On the Origin of Lunar Smooth Plains', *The Moon* **12**, 19–54.

Offield, T. W. and Pohn, H. A.: 1970, 'Lunar Crater Morphology and Relative Age Determination of Lunar Geologic Units, Part II, Applications', U.S. Geological Survey Prof. Paper 700-C, p. C 163–169.

O'Keefe, J. D. and Ahrens, T. J.: 1976, 'Impact Ejecta on the Moon', *Proc. 7th Lunar Sci. Conf.*, pp. 3007–3025.

Pike, R. J.: 1974, 'Ejecta from Large Craters on the Moon: Comments on the Geometric Model of McGetchin *et al.*,' *Earth Planet Sci. Letters* **23**, 265–271.

Pike, R. J.: 1976, 'Crater Dimensions from Apollo Data and Supplemental Sources', *The Moon* **15**, 463–477.

Pike, R. J.: 1977a, 'Size Dependence in the Shape of Fresh Impact Craters on the Moon', in D. J. Roddy, R. O. Pepin, and R. B. Merrill (eds.), *Impact and Explosion Cratering*, Pergamon Press, New York, pp. 489–509.

Pike, R. J.: 1977b, 'Apparent Depth/Apparent Diameter Relation for Lunar Craters', *Proc. 8th Lunar Sci. Conf.*, pp. 3427–3436.

Pike, R. J. and Wilhelms, D. E.: 1978, 'Secondary Impact Craters on the Moon: Topographic Form and Geologic Process' (abs.), *Lunar and Planetary Science IX*, pp. 907–909, Lunar and Planetary Institute, Houston, Tex.

Pohn, H. A. and Offield, T. W.: 1970, 'Lunar Crater Morphology and Relative Age Determination of Lunar Geologic Units, Part I, Classification', U.S. Geological Survey Prof. Paper 700-C, p. C 153–162.

Quaide, W. and Oberbeck, V.: 1975, 'Development of the Mare Regolith: Some Model Considerations', *The Moon* **13**, 27–55.

Roddy, D. J., Boyce, J. M., Colton, G. W., and Dial, A. L.: 1975, 'Meteor Crater, Arizona, Rim Drilling with Thickness, Structural Uplift, Diameter, Depth, Volume, and Mass-Balance Calculations', *Proc. 6th Lunar Sci. Conf.*, pp. 2621–2644.

Settle, M. and Head, J. W.: 1977, 'Radial Variation of Lunar Crater Rim Topography', *Icarus* **31**, 123–135.

Stoffler, D., Dence, M. R., Graup, G., and Abadian, M.: 1974, 'Interpretation of Ejecta Formations at the Apollo 14 and 16 Sites by a Comparative Analysis of Experimental Terrestrial, and Lunar Craters', *Proc. 5th Lunar Sci. Conf.*, pp. 137–150.

Stöffler, D., Gault, D. E. Wedekind, J., and Polkowski, G.: 1975, 'Experimental Hypervelocity Impact into Quartz Sand: Distribution and Shock Metamorphism of Ejecta', *J. Geophys. Res.* **80**, 4062–4077.

Swann, G. A. and Reed, V. S.: 1974, 'A Method for Estimating the Absolute Ages of Small Copernican Craters and its Application to the Determination of Copernican Meteorite Flux', *Proc. 5th Lunar Sci. Conf.*, pp. 151–158.

Tarasov, L. S., Nazarov, M. A., Shevaleevsky, I. D., Kidryashova, A. F., Gaverdovskaya, A. S., and Korina, M. I.: 1977, 'Mineralogy and Petrography of Lunar Rocks from Mare Crisium', (Preliminary Data), *Proc. 8th Lunar Science Conf.*, pp. 3333–3356.

Trask, N. J.: 1971, 'Geologic Comparisons of Mare Materials in the Lunar Equatorial Belt, Including Apollo 11 and Apollo 12 Landing Sites', U.S. Geological Survey Prof. Paper 750-D, p. D 138–148.

Ulrich, G. E., Moore, H. J., Reed, V. S., Wolfe, E. W., and Larson, K. B.: 1975, 'Distribution of Ejecta from South Ray Crater' (abs.), *Lunar Science VI*, pp. 832–834, Lunar and Planetary Institute, Houston, Tex.

Viktorov, V. V. and Stepenov, R. D.: 1960, *Inzh. Bs.* **28**, 87–96, transl. by M. I. Weinrich, SCLT-392, Sandia Corporation, Albuquerque, N.M., 1961.

Wasserburg, G. J., DiBrozolo, F. R., Papanastassiou, D. A., McCulloch, M. T., Huneke, J. C., Dymek, R. F., DePaolo, D. J., Chodos, A. A., and Albee, A. L.: 1978, 'Petrology, Chemistry, Age and Irradiation History of Luna 24 Samples', in *Mare Crisium: The View from Luna 24*, Pergamon Press, New York, pp. 657–678.

Whitaker, E. A.: 1972, 'Lunar Color Boundaries and Their Relationship to Topographic Features: A Preliminary Survey', *The Moon* **4**, 348–355.

Whitford-Stark, J. L. and Head, J. W.: 1978, 'Oceanus Procellarum: Preliminary Basalt Stratigraphy and Emplacement History' (abs.), *Lunar and Planetary Science IX*, Lunar and Planetary Institute, Houston, Tex., pp. 1250–1252.